

Safety assessment in reliability terms of bridges equipped with isolator devices

Original

Safety assessment in reliability terms of bridges equipped with isolator devices / Castaldo, Paolo; Miceli, Elena; Gino, Diego. - ELETTRONICO. - (2022), pp. 1-8. (3rd EUROPEAN CONFERENCE ON EARTHQUAKE ENGINEERING & SEISMOLOGY Bucarest 4-9 September 2022).

Availability:

This version is available at: 11583/2974136 since: 2023-01-09T14:21:53Z

Publisher:

Springer

Published

DOI:

Terms of use:

This article is made available under terms and conditions as specified in the corresponding bibliographic description in the repository

Publisher copyright

(Article begins on next page)

Safety assessment in reliability terms of bridges equipped with isolator devices

Paolo Castaldo – Politecnico di Torino, Turin, Italy, e-mail: paolo.castaldo@polito.it

Diego Gino – Politecnico di Torino, Turin, Italy, e-mail: diego.gino@polito.it

Elena Miceli – Politecnico di Torino, Turin, Italy, e-mail: elena.miceli@polito.it

Abstract: The study aims to determine the seismic reliability of bridges having multi-span continuous static scheme. The proposed modelling approach is able to account for vibrational modes of the reinforced concrete piers (supposed to be elastic) and assume an infinitely rigid deck supported by the isolator devices. The interaction between the piers and the abutment have been accounted for within the investigation. The randomness of the values assumed by friction coefficient on sliding surfaces is modelled adopting normal distribution. The non-linear dependence on the sliding velocity have been appropriately considered within the model adopted for friction coefficient. The seismic inputs adopted for the analysis have been selected in order to consider record-to-record variability selecting a set of natural accelerograms. Then, the fragility curves of both the pier and isolation system supporting the deck are determined. Finally, including the site information related to seismic hazard, the seismic reliability curves are derived and discussed.

Keywords: Risk analysis; composite bridges; concrete bridges, friction coefficient, structural safety.

1. Introduction

Bridges seismically isolated are largely employed to reduce the deck acceleration and forces that are transmitted to the piers during seismic events, as discussed by Jangid (2004), Ghobarah et al. (1988), Tsiavos et al. (2021a-b). More efficient infrastructures (Troisi et al. (2019), Troisi et al. (2022)) with reference to seismic reliability issues can have relevant and positive consequences within the surrounding territory and urban areas. One of the principal gains of adopting the friction pendulum isolation systems (FPS) results into have an isolation period which is not dependent from the mass associated to the superstructure (i.e., the deck in case of bridges) Zayas et al. (1990). In this investigation the randomness of the friction coefficient on sliding surfaces is accounted for according to law dependent from the velocity of motion Mokha et al. (1990), Constantinou et al. (1990) and Castaldo et al. (2020).

Several research have introduced the seismic reliability-base design (SRBD) for structures equipped with the FPS isolators, as for example Nassar et al. (2019). In Castaldo et al. (2021a), a methodology for seismic reliability assessment have been proposed including variability of the properties of the seismic isolation devices considering different structural configurations. Instead, Castaldo et al. (2021b) proposed the evaluation of optimal values of the friction coefficient with the aim to minimize the seismic response on the piers.

In investigation, the reliability analysis with reference to seismic actions of multi-span continuous bridges isolated with FPS devices is carried out considering a wide range of

configurations. The modelling approach for the isolated bridges consist of a five-degree-of-freedom (dof) system which rely to behaviour of the RC pier supposed as elastic. A further dof is considered to reproduce the response of the RC deck supported by FPS devices. The deck has been considered as infinitely rigid. The RC abutment is reproduced as a rigid structure. Adopting the mentioned above modelling approach the pier-abutment-deck interaction is included in the analysis, even if the backfill soil interaction with the abutment is neglected Mitoulis et al. (2012).

According to the approach, the relevant random variable associated to the friction coefficient have been considered. The Latin hypercube sampling method (LHS) is adopted according to Celarec et al. (2013). Furthermore, 30 natural seismic records having different characteristics has been properly scaled to various intensity levels according to the seismic hazard of the site of realization (i.e., L'Aquila (Italy)). The incremental dynamic analyses (IDAs) (Vamvatsikos et al. (2002)) have been performed in order to determine the response in terms of peak deck displacement and peak pier displacement. The results are useful to determine the seismic fragility curves Castaldo et al. (2018). The so far derived fragility curves help to evaluate the seismic reliability of bridges isolated with FPS devices Cornell et al. (2000) adopting the hazard curves of the site and a specific design reference life.

2. Modelling of dynamic response of continuous deck bridges

The seismic behaviour of the bridge is modelled by means of a six-degree-of-freedom (dof) scheme in which 5 dofs relates to the lumped masses of the pier and 1 additional dof is associated to the rigid RC deck Castaldo et al. (2021a). The friction pendulum devices (FPS) are located both on the top of the pier and of the abutment as shown by Figure 1.

The equations of motion derived in line to Figure 1 are the following:

$$\begin{aligned}
& m_d \ddot{u}_d(t) + m_d \ddot{u}_{p5}(t) + m_d \ddot{u}_{p4}(t) + m_d \ddot{u}_{p3}(t) + m_d \ddot{u}_{p2}(t) + m_d \ddot{u}_{p1}(t) + c_d \dot{u}_d(t) + f_b(t) + f_a(t) = -m_d \ddot{u}_g(t) \\
& m_{p5} \ddot{u}_{p5}(t) + m_{p5} \ddot{u}_{p4}(t) + m_{p5} \ddot{u}_{p3}(t) + m_{p5} \ddot{u}_{p2}(t) + m_{p5} \ddot{u}_{p1}(t) - c_{p5} \dot{u}_d(t) + c_{p5} \dot{u}_{p5}(t) + k_{p5} u_{p5}(t) - f_b(t) = -m_{p5} \ddot{u}_g(t) \\
& m_{p4} \ddot{u}_{p4}(t) + m_{p4} \ddot{u}_{p3}(t) + m_{p4} \ddot{u}_{p2}(t) + m_{p4} \ddot{u}_{p1}(t) - c_{p4} \dot{u}_{p5}(t) - k_{p5} u_{p5}(t) + c_{p4} \dot{u}_{p4}(t) + k_{p4} u_{p4}(t) = -m_{p4} \ddot{u}_g(t) \quad (1a,b,c,d,e,f) \\
& m_{p3} \ddot{u}_{p3}(t) + m_{p3} \ddot{u}_{p2}(t) + m_{p3} \ddot{u}_{p1}(t) - c_{p3} \dot{u}_{p4}(t) - k_{p4} u_{p4}(t) + c_{p3} \dot{u}_{p3}(t) + k_{p3} u_{p3}(t) = -m_{p3} \ddot{u}_g(t) \\
& m_{p2} \ddot{u}_{p2}(t) + m_{p2} \ddot{u}_{p1}(t) - c_{p2} \dot{u}_{p3}(t) - k_{p3} u_{p3}(t) + c_{p2} \dot{u}_{p2}(t) + k_{p2} u_{p2}(t) = -m_{p2} \ddot{u}_g(t) \\
& m_{p1} \ddot{u}_{p1}(t) - c_{p1} \dot{u}_{p2}(t) - k_{p2} u_{p2}(t) + c_{p1} \dot{u}_{p1}(t) + k_{p1} u_{p1}(t) = -m_{p1} \ddot{u}_g(t)
\end{aligned}$$

where u_d is the relative displacement of the deck evaluated at the top of the pier, u_{pi} ($i=1:5$), denotes the relative displacement of the i -th mass of the pier referred to the lower one, m_d represents the mass of the deck, m_{pi} is the mass of the i -th lumped mass of the pier, while k_{pi} is the related stiffness. The coefficient of viscous damping of the devices and of the pier masses are, respectively, c_d and c_{pi} ; t is the time variable. With reference to the resisting forces that arises within the FPS bearings, these are denoted respectively as $f_a(t)$ and $f_p(t)$. Such kind of reactions can be derived as follows according to Zayas et al. (1990):

$$\begin{aligned}
f_a(t) &= \frac{m_d g}{2} \left[\frac{1}{R_a} \left(u_d(t) + \sum_{i=1}^5 u_{pi} \right) + \mu_a \left(\dot{u}_d + \sum_{i=1}^5 \dot{u}_{pi} \right) \operatorname{sgn} \left(\dot{u}_d + \sum_{i=1}^5 \dot{u}_{pi} \right) \right] \\
f_p(t) &= \frac{m_d g}{2} \left[\frac{1}{R_p} u_d(t) + \mu_p (\dot{u}_d) \operatorname{sgn}(\dot{u}_d) \right]
\end{aligned} \quad (2a,b)$$

In Eq.(2a,b) R_a and R_p are the radii of curvature of the FPS devices which is placed on the abutment and on the pier. The same values are adopted for both R_a and R_p ; the stiffness of the deck, coming from the elastic component of the reaction force over the FPS, is evaluated as

$k_d = W / R = m_d g / R$; g is the gravity constant; μ the sliding friction coefficient of the isolator on the abutment or of the isolator on the pier, $\dot{u}(t)$ is the sliding velocity. Finally, $\text{sgn}(\cdot)$ denotes the sign function.

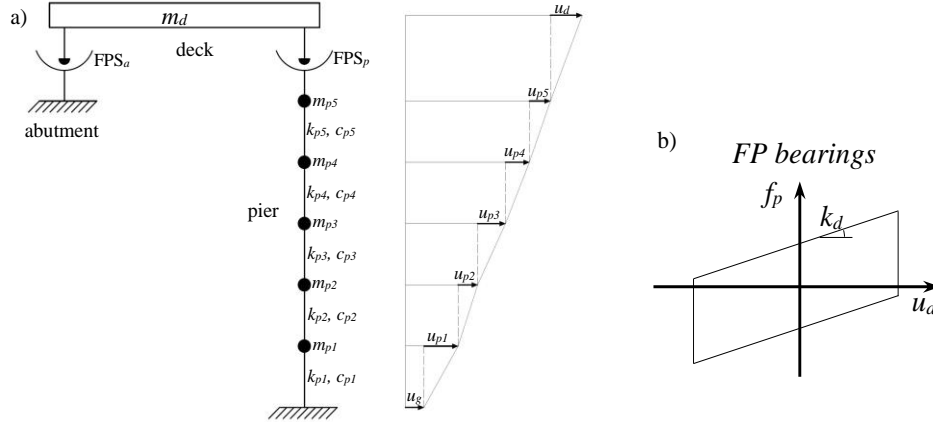


Figure 1 – Modelling approach for the bridge isolated by FPS devices (a) – 6 dofs; response of the FPS on the top of the pier/abutment (b).

The fundamental period of the deck isolated with FPS devices can be expressed as:

$$T_d = 2\pi\sqrt{m_d / k_d} = 2\pi\sqrt{R / g} .$$

The present investigation considers the dependency of the sliding friction coefficient on the velocity of motion according to Mokha et al. (1990) and Constantinou et al. (2007):

$$\mu(\dot{u}_d) = f_{\max} - (f_{\max} - f_{\min}) \cdot \exp(-\alpha|\dot{u}_d|) \quad (3)$$

where f_{\max} and f_{\min} define, respectively, the sliding friction at large and low velocity, α governs the transition mode from large to low velocities. Experimental results suggest assuming $f_{\max} = 3f_{\min}$ and $\alpha = 30$ Castaldo et al. (2018). Dividing Eqs.(1) by the value of m_d , which represents the deck mass, dimensionless relationships can be derived according to Castaldo et al. (2021b).

3. Probabilistic model for input random variables

3.1. Seismic action

In line with the Performance Based Earthquake Engineering approach (PBEE) Porter (2004), this investigation adopts specific values of intensity measure (IM) to scale a set of 30 natural records. The mentioned records are selected from different databases (i.e., PEER, ITACA, ISESD-Internet Site for European Strong-Motion Data), see also Castaldo et al. (2021b). The intensity measure herein adopted is the spectral-displacement $S_D(T_d, \xi_d)$ determined in concomitance of the isolated period of the bridge system, $T_d = 2\pi / \omega_d$ with a value of the damping ratio ξ_d set equal to zero Castaldo et al. (2021)b, Iervolino et al. (2005). For instance, the IM is denoted from now on as $S_D(T_d)$ and a range of variability between 0.10m and 0.45m (see Table 2) is considered to realize the IDAs according to the seismicity of the considered site (L'Aquila (Italy)), NTC18 (2018).

Table 1. Selection of values associated to the intensity measure $s_D(T_d)$.

IM	1	2	3	4	5	6	7	8
$s_D(T_d)$ [m]	0.10	0.15	0.20	0.25	0.30	0.35	0.40	0.45

3.2. Friction coefficient on sliding surfaces

With reference to the uncertainty associated to the friction coefficient Wei et al. (2020), Castaldo et al. (2017), the value of f_{\max} can be probabilistically modelled according to a normal PDF truncated between 0.5% and 5.5% with a mean value equal to 3%, Castaldo et al. (2015). The, the LHS method has been adopted to generate 15 different samples.

Concerning the structural properties, a large parametric analysis has been realized considering different types of bridges. In particular, the isolated superstructure period T_d varies between 1s and 4s; the RC pier period T_p equal to 0.05s; $\lambda = \sum_{i=1,5} m_{pi} / m_d$, denotes the overall mass ratio related to the sum of the i-th mass ratios (assumed equal), ranges between 0.1, 0.15 and 0.2.

4. Methodology to perform Incremental Dynamic Analysis

Considering all the possible combinations related to deterministic (T_d , λ and T_p) and random parameters, the set of Eqs. (1) have been solved for the 30 seismic records. The latter has been scaled to 8 values of $s_D(T_d)$ as reported in Table 1. Then, the IDAs (De Iuliis et al. (2012)) are performed using the Matlab® platform.

The outputs of the mentioned above IDAs have been derived assuming the following engineering demand parameters (EDPs): $u_{d,\max}$ and $u_{p,\max} = \left(\sum_{i=1}^5 u_{pi} \right)_{\max}$. In this way, a set of samples is collected for each EDP at the fixed level of IM. The samples of the EDPs are assumed to be in line with a probabilistic lognormal distribution. The statistical parameters associated to the lognormal distribution can estimated for each EDP by calculating the sample lognormal mean $\mu_{\ln}(EDP)$ and the sample lognormal standard deviation, $\sigma_{\ln}(EDP)$ according to the maximum likelihood Castaldo et al. (2018), Castaldo et al. (2022), Troisi et al. (2021) and Gino et al. (2016). Finally, the relevant 50th, 84th and 16th percentiles related to the specific PDF can be derived Castaldo et al. (2015).

5. Evaluation of the seismic fragility

The evaluation of the seismic reliability requires the determination of the seismic fragility curves introducing the probabilities P_f of exceeding specific limit states (LSs) with reference to each level of the IM. Concerning the LS thresholds associated to the system of isolation, nine values of the in-plan radius of the single concave surface of FPD devices have been considered Castaldo et al. (2017), as shown in the Table 2. Different values are considered in order to define the reliable dimension. With reference to the pier, four LSs (LS1, LS2, LS3 and LS4) are considered referring to “fully operational”, “operational”, “life safety” and “collapse prevention”, in line with SEAOC Vision 2000 (1995). The values are specific for reinforced concrete structural systems. The adopted parameter to characterize the LS is the pier drift index (PDI) (see Table 3) Castaldo et al. 2020.

	1	2	3	4	5	6	7	8	9
r [m]	0.10	0.15	0.20	0.25	0.30	0.35	0.40	0.45	0.50

	LS1 Fully Operational	LS2 Operational	LS3 Life Safety	LS4 Near collapse
PDI_{IB}	$PDI_{IB}=0.23\%$	$PDI_{IB}=0.5\%$	$PDI_{IB}=0.83\%$	$PDI_{IB}=1.67\%$
P_f	$5 \cdot 10^{-1}$	$1.6 \cdot 10^{-1}$	$2.2 \cdot 10^{-2}$	$1.5 \cdot 10^{-3}$

Next, the probabilities P_f related to the exceedance of the mentioned above LSs with regard to the isolation system (i.e., of the deck) and to the RC substructure/pier have been determined. The Figure 2 and the Figure 3 relates to the fragility curves of the isolation system evaluated for the values of T_p and T_d , for each LS and each value of λ . It can be highlighted that the seismic fragility decreases with the increasing of T_d . In case of bridges decks with low T_d , an increase of T_p carry to small increase of the seismic fragility.

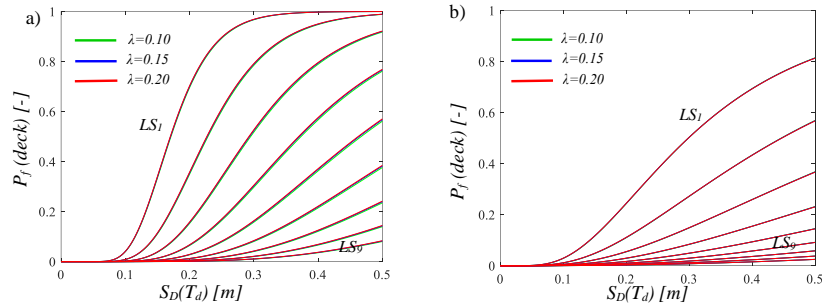


Figure 2 – Seismic fragility curves related to the deck for $T_p=0.05s$ and a) $T_d=1s$, b) $T_d=4s$.

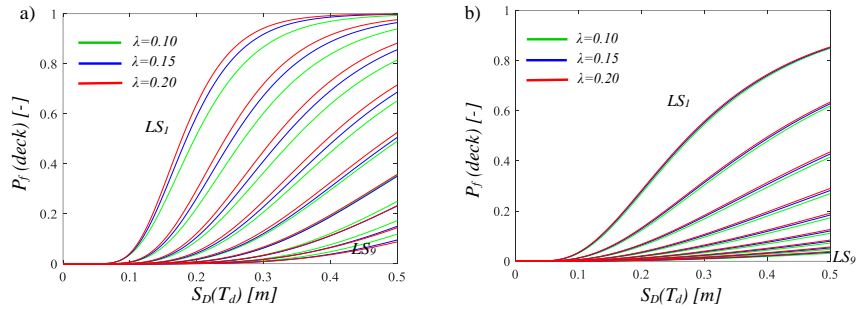


Figure 3 - Seismic fragility curves related to the deck for $T_p=0.2s$ and a) $T_d=1s$, b) $T_d=4s$.

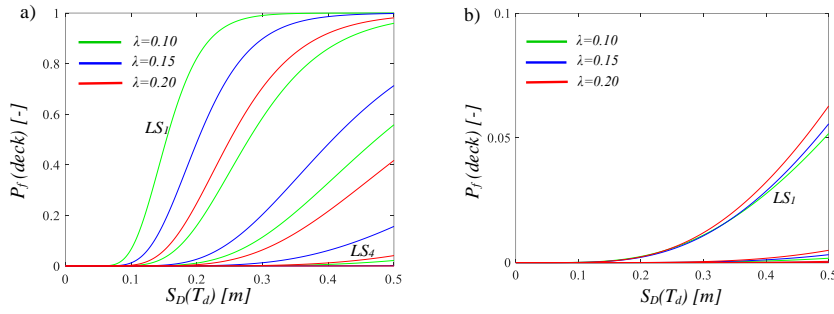


Figure 4 - Seismic fragility curves related to the pier for $T_p=0.05s$ and a) $T_d=1s$, b) $T_d=4s$.

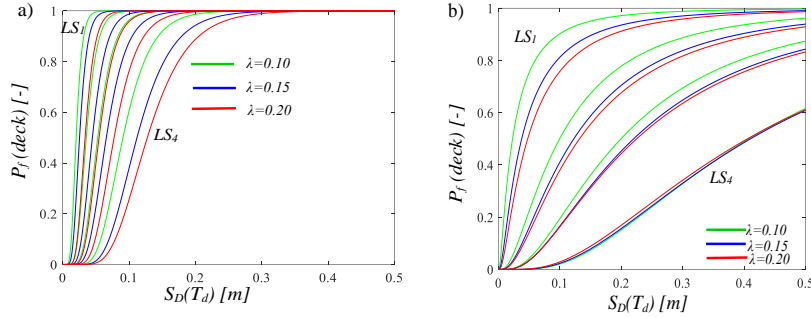


Figure 5 - Seismic fragility curves related to the pier for $T_p=0.2s$ and a) $T_d=1s$, b) $T_d=4s$.

6. From seismic fragility to seismic reliability

By means the combination of the seismic fragility curves with the site specific (L'Aquila (Italy)) seismic hazard curves, it is possible to determine the mean annual rates of exceedance for specific LSs. In particular, adopting the Poisson probabilistic model, the probabilities of exceedance over 50 years of design service life (Vamvatsikos et al. (2002)) can be evaluated. The seismic reliability curves associated to the isolation devices are derived, as reported by Figure 6. The mentioned above curves may be used with the aim to perform preliminary design (i.e., determining the radius in plan, r ,) of the FPSs.

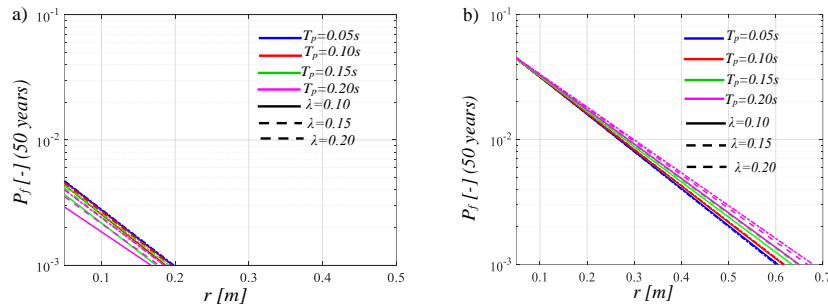


Figure 6 - Seismic reliability curves related to the deck for a) $T_d=1s$, b) $T_d=4s$.

7. Conclusions

The investigation focuses on the evaluation of the seismic reliability of bridges decks having multi-span continuous static scheme in presence of single concave friction pendulum (FPS) isolation system. In particular, a large parametric analysis related to both the properties of the isolators and of the bridge have been carried out.

In particular, the randomness of the friction coefficient on sliding surfaces has been modelled by means effective probabilistic distribution. Firstly, a group of 30 natural records have been considered to take into account the uncertainties related to the seismic input. Then, the natural records have been scaled to different values of the intensity measure according to the site-specific information. Secondly, the fragility curves associated to both the continuous deck and the RC pier, have been derived and used to determine the seismic reliability including also the information related to the seismic hazard of the construction site. As a result of the fragility analysis, it can be recognised that the seismic reliability of the deck decreases when the value r (i.e., radius of curvature of the FPS isolator) increase. This is because of the relevant seismic hazard of the considered construction site. With reference to the pier, the seismic reliability decreases in case of high natural periods and high isolated periods because of the randomness of the friction coefficient on sliding surfaces and of the relevant seismic hazard of the construction site.

References

- Castaldo P, Alfano G (2020) Seismic reliability-based design of hardening and softening structures isolated by double concave sliding devices. *Soil Dynamics and Earthquake Engineering* 129, 105930.
- Castaldo P, Amendola G (2021) Optimal DCFP bearing properties and seismic performance assessment in nondimensional form for isolated bridges, *Earthquake Engineering and Structural Dynamics* 50(9), 2442–2461.
- Castaldo P, Amendola G (2021) Optimal Sliding Friction Coefficients for Isolated Viaducts and Bridges: A Comparison Study. *Structural Control and Health Monitoring* 28(12).
- Castaldo P, Amendola G, Ripani M (2018) Seismic fragility of structures isolated by single concave sliding devices for different soil conditions, *Earthquake Engineering and Engineering Vibration* 17(4), 869-891.
- Castaldo P, Gino D, Marano G, Mancini G (2022) Aleatory uncertainties with global resistance safety factors for non-linear analyses of slender reinforced concrete columns, *Engineering Structures*, 255, 113920, S0141-0296(22)00078-5.
- Castaldo P, Palazzo B, Ferrentino T, Petrone G (2017) Influence of the strength reduction factor on the seismic reliability of structures with FPS considering intermediate PGA/PGV ratios, *Composites Part B: Engineering* 115, 308-315.
- Castaldo P, Tubaldi E (2015) Influence of FPS bearing properties on the seismic performance of base-isolated structures. *Earthquake Engineering and Structural Dynamics* 44(15), 2817–2836.
- Castaldo P, Tubaldi E (2018) Influence of Ground Motion Characteristics on the Optimal Single Concave Sliding Bearing Properties for Base-isolated Structures, *Soil Dynamics and Earthquake Engineering* 104, 346-64.
- Celarec D, Dolšek M (2013) The impact of modelling uncertainties on the seismic performance assessment of reinforced concrete frame buildings, *Engineering Structures* 52, 340-354.
- Constantinou MC, Mokha A, Reinhorn AM (1990) Teflon Bearings in Base Isolation. II: Modeling. *Journal of Structural Engineering* 116(2), 455-474.
- Cornell CA, Krawinkler H (2000) Progress and challenges in seismic performance assessment, *PEER Center News* 4(1), 1-3.
- De Iuliis M, Castaldo P (2012) An energy-based approach to the seismic control of one-way asymmetrical structural systems using semi-active devices. *Ingegneria Sismica-International Journal of Earthquake Engineering* 29(4), 31-42.
- deformation demand for a structure isolated using friction-pendulum sliding bearings. *Structures* 31, 1041-1052.
- Ghobarah A, Ali HM (1988) Seismic Performance of Highway Bridges. *Engineering Structures* 10(3), 157-66.
- Gino D, Bertagnoli G, Mancini G (2016) Effect of endogenous deformations on composite bridges, *Recent Progress in Steel and Composite Structures - Proceedings of the 13th International Conference on Metal Structures, ICMS 2016*, pp. 287-298. 15-17June, Zielona Gora, Poland.
- Iervolino I, Cornell CA (2005) Record selection for nonlinear seismic analysis of structures, *Earthquake Spectra* 21(3), 685-713.
- Jangid RS (1988) Seismic Response of Isolated Bridges. *Journal of Bridge Engineering* 9(2), 156-166.

- Math Works Inc. (1997) MATLAB-High Performance Numeric Computation and Visualization Software. User's Guide. Natick (MA) USA.
- Mitoulis SA (2012) Seismic design of bridges with the participation of seat-type abutments, *Engineering Structures* 44, 222-233.
- Mokha A, Constantinou MC, Reinhorn AM (1990) Teflon Bearings in Base Isolation. I: Testing. *Journal of Structural Engineering* 116(2), 438-454.
- Nassar M, Guizani L, Nollet MJ, Tahan A (2019) A probability-based reliability assessment approach of seismic base-isolated bridges in cold regions. *Engineering Structures* 197, 109353.
- NTC18 (2018) Norme tecniche per le costruzioni. *Gazzetta Ufficiale* del 20.02.18, DM 17.01.18, Ministero delle Infrastrutture.
- SEAOC Vision 2000 (1995). Committee. Performance-based seismic design engineering. Report prepared by Structural Engineers Association of California, Sacramento, CA.
- Troisi R, Alfano G (2019) Towns as Safety Organizational Fields: An Institutional Framework in Times of Emergency. *Sustainability* 11, 7025. DOI:10.3390/su11247025.
- Troisi R, Castaldo P (2022) Technical and organizational challenges in the risk management of road infrastructures, *Journal of Risk Research*, DOI:10.1080/13669877.2022.2028884.
- Troisi R, Di Nauta P, Piciocchi P (2021) Private corruption: An integrated organizational model. *European Management Review*.
- Tsiavos A, Schlatter D, Markic T, Stojadinovic B (2021b) Shaking table investigation of inelastic
- Tsiavos A, Sextos A, Stavridis A, Dietz M, Dihoru L, Alexander NA (2021a) Experimental investigation of a highly efficient, low-cost PVC-Rollers Sandwich (PVC-RS) seismic isolation. *Structures* 33, 590-1602.
- Vamvatsikos D, Cornell CA (2002) Incremental dynamic analysis. *Earthquake Engineering and Structural Dynamics* 31(3), 491-514.
- Wei B, Fu Y, Li S, Jiang L, He W (2020) Scaling errors of a seismic isolation system with a shear key, *Soil Dynamics and Earthquake Engineering*, 139, 106382.
- Zayas V, Low S, Mahin S (1990) A simple pendulum technique for achieving seismic isolation. *Earthquake Spectra* 6(2), 317-333.